VERSITA
Electrical, Control and Communication Engineering
doi: 10.2478/ecce-2013-0009
2013 / 3

# Conducted EMI of Switching Frequency Modulated Boost Converter

Deniss Stepins (*Researcher, Riga Technical University*)

***Abstract* – In this paper conducted electromagnetic interference (EMI) of boost converter with switching frequency modulation (SFM) is theoretically analyzed in details. In the analysis line impedance stabilization network parameters, power inductor and input filtering capacitor parameters are taken into account. The analysis shows that the conducted EMI attenuation due to the use of SFM depends not only on modulation index as it is assumed in numerous research papers, but also on central switching frequency. Useful expressions to numerically calculate SFM boost converter conducted EMI spectrum and attenuation due to the use of triangular and sawtooth modulation waveforms are derived. Additionally experimental verification of the theoretical results is performed using a superheterodyne spectrum analyzer. Moreover a procedure for the choice of optimum SFM parameters (modulation waveform, frequency deviation and modulation frequency) to get maximum conducted EMI attenuation is proposed.**

***Keywords* – Electromagnetic interference, switched-mode power supply, frequency modulation.**

## I. Introduction

Nowadays switch-mode power converters (SMPC) are often used in many electronic devices to convert electric power with high efficiency. High levels of electromagnetic interference (EMI) both conducted and radiated are still one of the major disadvantages of SMPC. Thus, much attention is usually focused on EMI reduction when designing a SMPC [1-3].

To suppress EMI, filtering, shielding, soft-switching etc. are usually used in practice. However, over the last decade so called spread-spectrum technique has been extensively studied by researchers all over the world and used for the EMI reduction in SMPC including power factor correctors (PFC), lighting equipment electronic ballasts, inverters, etc. [4-7]. Noticeable suppression of peak EMI levels can be simply obtained by the modulation of switching frequency $f_{sw}$ using simple periodic modulating waveforms (such as sine, triangle, sawtooth, etc) thus spreading the spectrum of SMPC voltages and currents [8],[9]. Switching frequency modulation (SFM) can reduce not only conducted but radiated EMI as well [11].

Although numerous research papers [6-11] are devoted to SMPC conducted EMI reduction with periodic SFM, usually the analysis includes only the investigation of spectra of rectangular pulse trains (representing power component voltages) or power component currents (such as power inductor current). However the conducted EMI noise voltage waveforms highly differ from the power component voltages and currents waveforms [12]. Thus the analysis presented in the papers can omit several important details of the effect of SFM parameters on conducted EMI attenuation.

In this paper a comprehensive theoretical analysis of conducted EMI of SFM SMPC is presented. In the analysis the effect of line impedance stabilization network (LISN) and input EMI filter parameters is also taken into account. Moreover the expressions to calculate SFM SMPC EMI spectrum and EMI attenuation due to the use of triangular and sawtooth modulation waveforms are derived. Additional experimental verification is performed and a procedure for the choice of optimum SFM parameters to get maximum EMI attenuation is proposed.

## II. Theoretical Analysis of EMI of SMPC without SFM

In this chapter the conducted EMI spectrum without SFM will be considered first. It is rather well known from the power electronics that for EMI measurements LISN and EMI spectrum analyzer are used as shown in Fig.1. A spectrum analyzer with specified resolution bandwidth (RBW) and detector type is connected to the LISN radio-frequency measurement output to analyze conducted EMI spectrum in the specified frequency range (e.g. 9kHz-30MHz).

During the design process it is of importance to predict EMI spectrum theoretically. Theoretical analysis and prediction of conducted EMI of SMPC without SFM has been performed in various papers, e.g. [12] - [16]. Usually EMI is analyzed using computer simulation and fast Fourier transform (FFT) to calculate EMI spectrum. However several papers [12], [16] propose simple analytical models for EMI analysis and prediction in SMPC without SFM.

In this paper a boost DC-DC converter operating in continuous conduction mode (CCM) is chosen for the analysis. In Fig.2 boost SMPC with input filtering capacitor $C_{in}$ and LISN is shown. To simplify the analysis only non-idealities of $C_{in}$ and power inductor will be taken into account. Since conducted EMI is of interest, LISN radio-frequency measurement output voltage $V_{LISN}$ will be analyzed in the frequency domain. $V_{ens}$ should be derived first in order to calculate $V_{LISN}$ spectrum transfer function $K_{EMI}(f)$ between $V_{LISN}$ and an equivalent noise source [12], [16].

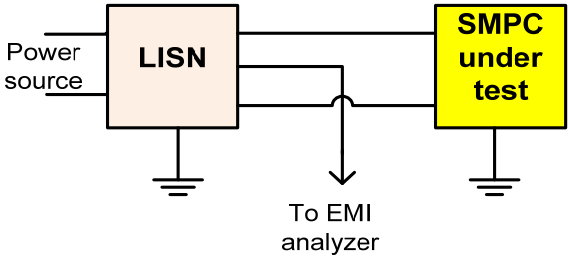


Fig.1. Typical conducted EMI measurement setup.

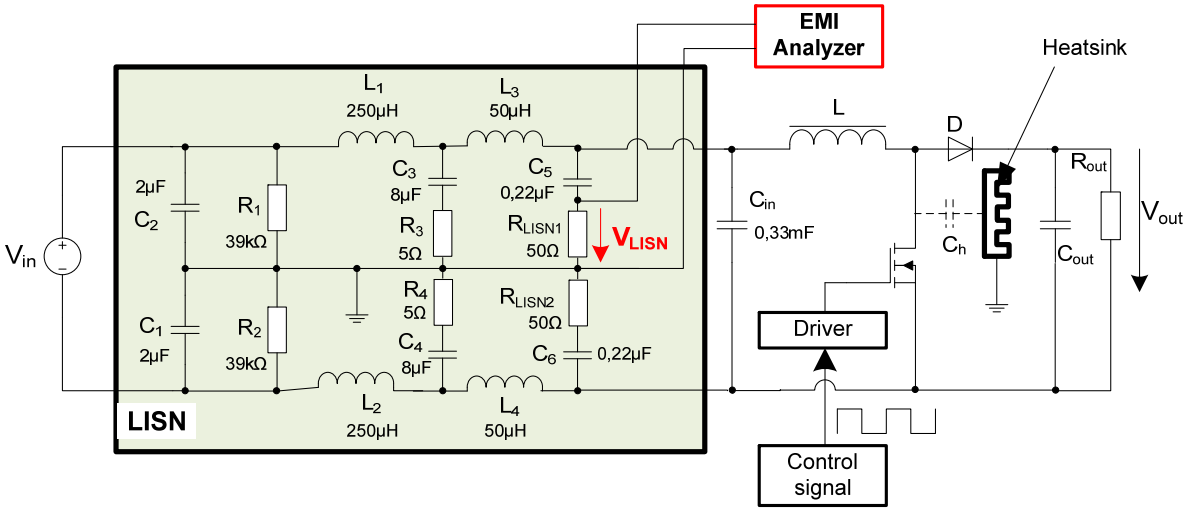


Fig.2. Boost SMPC schematic diagram with LISN.

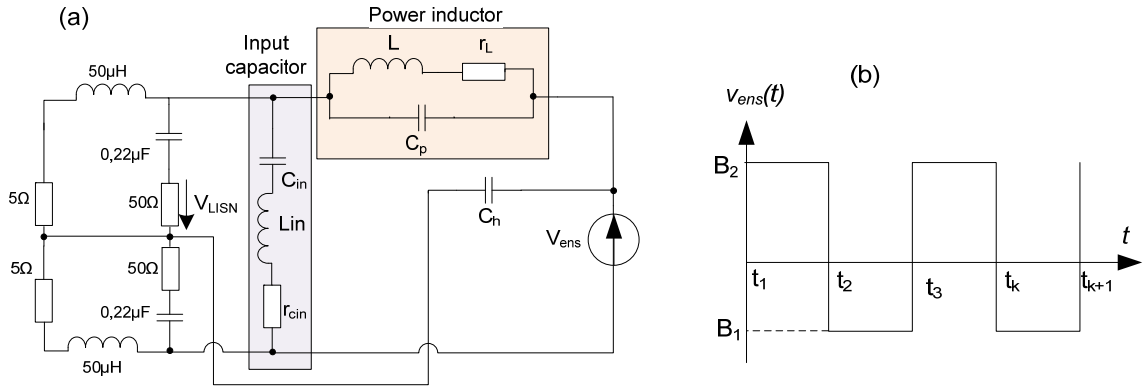


Fig.3.(a) simple boost SMPC EMI model (slightly modified version taken from [12]), (b) equivalent noise source voltage waveform.

For this purpose a slightly modified simple EMI model taken from [12] is used as shown in Fig.3(a). Using the model the transfer function between $V_{ens}$ and $V_{LISN}$ can be derived:

$$\underline{K}_{EMI}(f) = \frac{50}{50+\underline{Z}_{C5}}\left(\frac{\underline{Z}_e}{\underline{Z}_{Ch}+\underline{Z}_e} - \frac{\underline{Z}_{Cin}}{2(\underline{Z}_{Cin}+\underline{Z}_L)}\right), \quad (1)$$

where

$$\underline{Z}_e = (25+\underline{Z}_{C5}/2)\cdot(5+\underline{Z}_{L3})/(55+\underline{Z}_{C5}+\underline{Z}_{L3}),$$

but $\underline{Z}_{C5} = 1/(j\cdot 2\pi f\cdot C_5)$,

$\underline{Z}_{Ch} = 1/(j\cdot 2\pi f\cdot C_h)$

and $\underline{Z}_{L3} = j\cdot 2\pi f\cdot L_3$,

real input capacitor complex impedance

$$\underline{Z}_{Cin} = \frac{1}{j2\pi f C_{in}} + j2\pi f L_{Cin} + r_{Cin} \quad (2)$$

and real power inductor complex impedance [17]

$$\underline{Z}_L = \frac{r_L + j2\pi f L}{1-(2\pi f)^2 L C_p + j2\pi f r_L C_p} \quad (3)$$

The transfer function $K_{EMI}(f)$ for different values of parasitic capacitance $C_h$ between MOSFET drain and a grounded heatsink is shown in Fig.4.

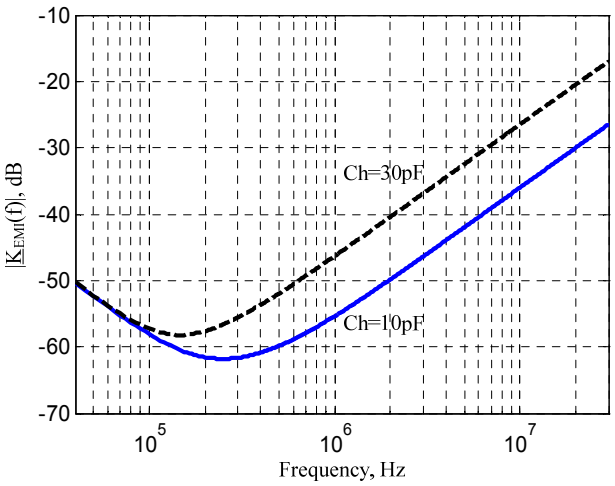


Fig.4. Transfer function $K_{EMI}$(f) for different $C_h$.

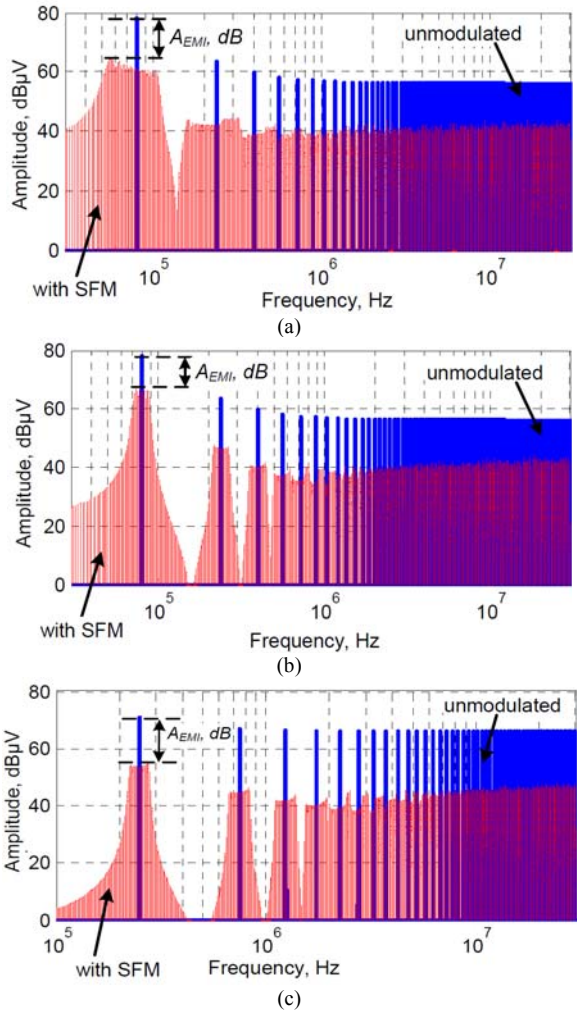


Fig.5. Spectrum of unmodulated and SFM $V_{LISN}$: (a) $f_{sw}$=80kHz, $f_m$=1kHz, $\Delta f_{sw}$=30kHz; (b) $f_{sw}$=80kHz, $f_m$=1kHz, $\Delta f_{sw}$=10kHz; (c) $f_{sw}$=250kHz, $f_m$=1kHz, $\Delta f_{sw}$=30kHz. Other parameters: $D$=0.5, $V_{in}$=4V, $m(t)$ is sawtooth.

Thus $V_{LISN}$ spectrum can be calculated as

$$S_{VLISN}(f) = S_{Vens}(f) \cdot \underline{K}_{EMI}(f), \tag{4}$$

where $V_{ens}$ spectrum $S_{Vens}(f)=2d_n$ (where $d_n$ are Fourier series complex coefficients) according to

$$d_n = \frac{1}{T_{sw}} \int_0^{T_{sw}} v_{ens}(t) e^{-j2\pi n f_{sw} t} dt = \\ = \frac{1}{T_{sw}} \left[ \int_0^{DT_{sw}} B_2 e^{-j2\pi n f_{sw} t} dt + \int_{DT_{sw}}^{T_{sw}} B_1 e^{-j2\pi n f_{sw} t} dt \right] = \\ = \frac{\left[ B_2 \left( e^{-j2\pi nD} - 1 \right) + B_1 \left( e^{-j2\pi n} - e^{-j2\pi nD} \right) \right]}{j2\pi n}, \tag{5}$$

where $D$ is duty ratio, $T_{sw}$ is switching period, $f_{sw}$ is switching frequency. For boost SMPC $B_2=V_{out}$-$V_{in}$ and $B_1$=-$V_{in}$ [16].

The calculated conducted EMI ($V_{LISN}$ spectrum) when $D$=50% is shown in Fig.5. It can be seen that the spectrum consists of discrete harmonics of $f_{sw}$. The 1st harmonic amplitude is the highest.

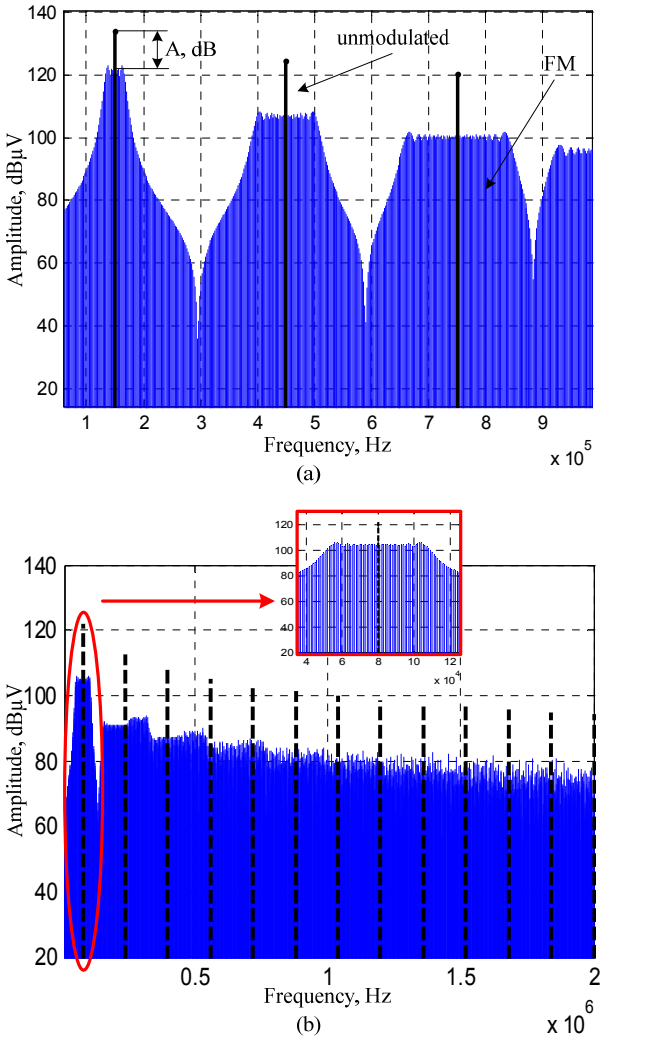


Fig.6. Spectrum of unmodulated and SFM $V_{ens}$: (a) $f_{sw}$=150kHz, $f_m$=2kHz, $\Delta f_{sw}$=20kHz, $m(t)$ is sawtooth; (b) $f_{sw}$=80kHz, $f_m$=1kHz, $\Delta f_{sw}$=30kHz, $m(t)$ is sawtooth. Other parameters: $D$=0.5, $B_1$ = –1V, $B_2$ = 1V.

## III. Theoretical Analysis of EMI of SMPC with SFM

When the SFM is used then $V_{ens}$ and $V_{LISN}$ spectra are more difficult to calculate. For sinusoidal SFM $V_{ens}$ spectrum can be obtained using the Bessel functions as follows [7]

$$S_{Vens}(f) = \sum_{n=-\infty}^{\infty} 2d_n \cdot [J_o(n\beta) \cdot \delta(f - nf_{sw}) + \sum_{k=1}^{\infty} J_k(n\beta) \cdot \\ \cdot \{\delta(f - nf_{sw} - kf_m) + (-1)^k \cdot \delta(f - nf_{sw} + kf_m)\}], \tag{6}$$

where $J_k$ is $k$th order Bessel function, $\beta$ is the modulation index and $f_m$ is modulation frequency. For other modulation waveforms e.g. sawtooth, triangular, etc. the spectrum calculation is more difficult [11]. Usually to calculate the spectrum of SFM signal, FFT is used as it was done e.g. in [9]. However, as such FFT requires a lot of computation time and power. Thus in this paper simple expressions to calculate EMI spectrum are derived. For this purpose Fourier series can be used, assuming that when $T_m/T_{sw}$ is an integer number then SFM signal is periodic with modulation period $T_m$ [11].

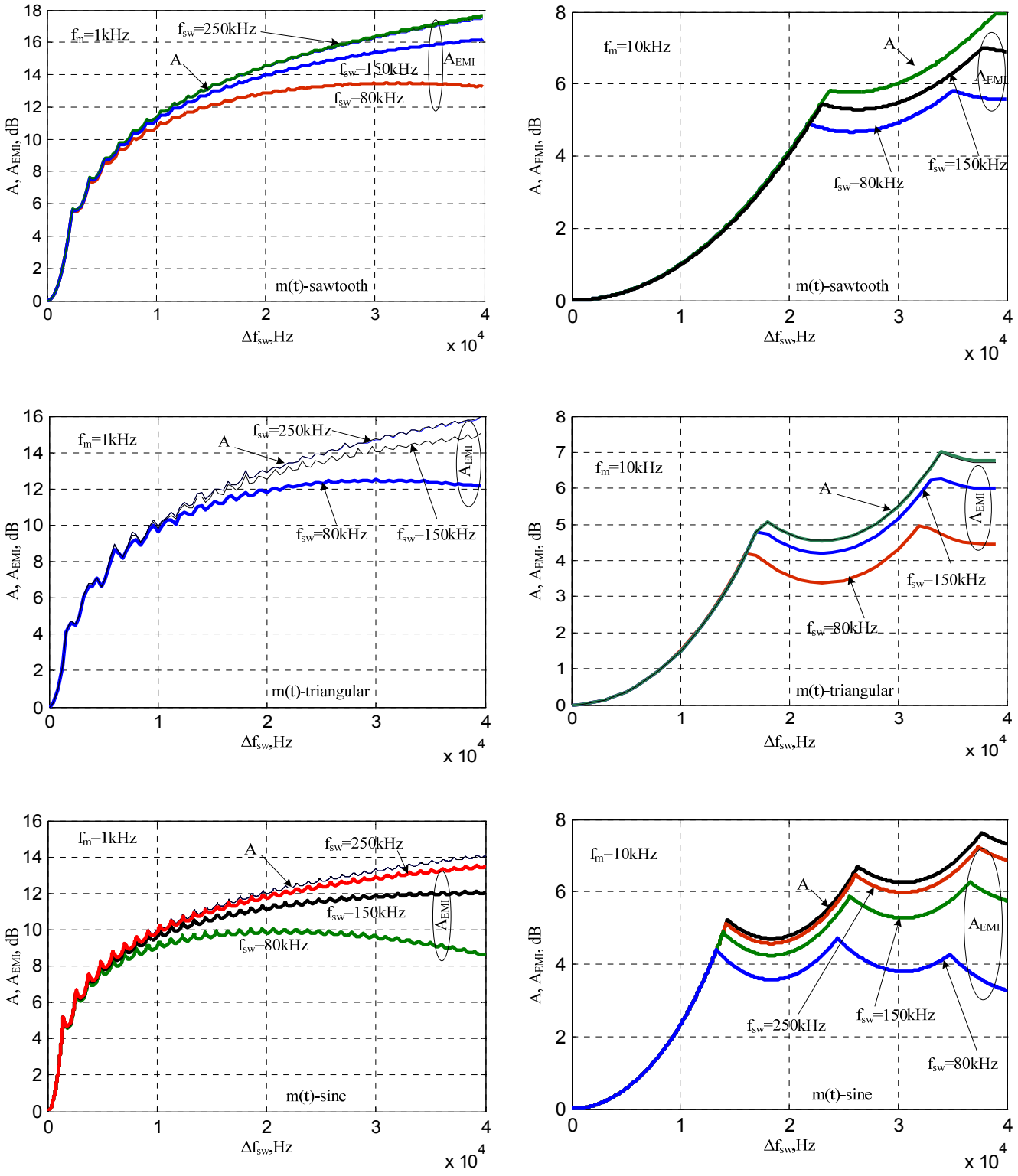


Fig.7. *A* and $A_{EMI}$ versus $\Delta f_{sw}$ for different *m(t)* and $f_{sw}$.

Complex Fourier series coefficients for SFM $V_{ens}$ – Fig.3(b).

$$d_{sn} = \frac{1}{T_m}\left[ B_2 \int_{t_1}^{t_2} e^{-j2\pi n f_m t} dt + B_1 \int_{t_2}^{t_3} e^{-j2\pi n f_m t} dt + ... + \right.$$

$$\left. + B_2 \int_{t_k}^{t_{k+1}} e^{-j2\pi n f_m t} dt + .... + B_1 \int_{t_N}^{t_{N+1}} e^{-j2\pi n f_m t} dt \right] =$$

$$= -\frac{B_2}{j2\pi n} \sum_{i=1}^{N/2} [e^{-j2\pi n f_m t_{2i}} - e^{-j2\pi n f_m t_{2i-1}}] -$$

$$-\frac{B_1}{j2\pi n} \sum_{i=1}^{N/2} [e^{-j2\pi n f_m t_{2i+1}} - e^{-j2\pi n f_m t_{2i}}] \qquad (7)$$

where an integer number $N=2f_{sw}/f_m$. $t_k$ are the time instants at which $V_{ens}$ crosses zero – Fig.3(b). They can be calculated by solving trigonometric equation [11]

$$\cos(2\pi f_{sw} \cdot t + \theta(t)) = 0\,, \qquad (8)$$

where the time dependent phase angle [6] is

$$\theta(t) = 2\pi \int_0^t \Delta f_{sw} \cdot m(\tau) d\tau\,, \qquad (9)$$

but $m(t)$ is the modulation signal with unitary amplitude.
Solution of (8) with respect to $t$ produces a set of simple analytical expressions of $t_k$ calculation for sawtooth SFM

$$t_k = \frac{-f_{sw\min} + \sqrt{f_{sw\min}^2 + \Delta f_{sw} \cdot (2k-1)/T_m}}{2\Delta f_{sw}/T_m} \qquad (10)$$

and for triangular SFM

$$t_k = \begin{cases} = \dfrac{-f_{sw\min} + \sqrt{f_{sw\min}^2 + \Delta f_{sw} \cdot 2k/T_m}}{4\Delta f_{sw}/T_m} \\ at \quad 0 \le t \le T_m/2, \\ = \dfrac{f_{sw} + 3\Delta f_{sw} - \sqrt{(f_{sw} + 3\Delta f_{sw})^2 + 4\Delta f_{sw} \cdot (\frac{k}{2} + \beta)}}{4\Delta f_{sw}/T_m} \\ at \quad T_m/2 < t \le T_m \end{cases} \qquad (11)$$

where $f_{swmin}=f_{sw}-\Delta f_{sw}$ and $\beta=\Delta f_{sw}/f_m$.

Derived expressions (7), (10) and (11) can be simply used to numerically calculate $V_{ens}$ and $V_{LISN}$ spectra in SMPC with triangular and sawtooth SFM. Using the expressions and Matlab code the spectra can be calculated just within a few seconds. As an example unmodulated and SFM boost SMPC theoretical spectra of $V_{ens}$ are shown in Fig.6. In turn, in Fig.5 calculated conducted EMI spectra ($V_{LISN}$ spectra) are shown for different $f_{sw}$. As it can be seen from the figures SFM leads to noticeable decrease in amplitudes of unmodulated $f_{sw}$ harmonics. It is interesting to observe that when adjacent sidebands do not overlap then the sidebands are symmetrical with respect to $f_{sw}$ and its harmonics in $V_{ens}$ spectrum. However in the case of $V_{LISN}$ spectrum, the sidebands are asymmetrical when $f_{sw}$=80kHz. This is because the transfer function between $V_{ens}$ and $V_{LISN}$ depends on frequency (Fig.4). In fact the sideband asymmetry is also observed in SFM electronic ballast output current [5].

Effectiveness of the use of SFM is characterized by a parameter called attenuation which is the difference in ($dB$) between maximum amplitude of unmodulated and SFM spectra in the frequency range of interest [9], [18]. In the literature the researchers usually consider only attenuation ($A$) of amplitudes of unmodulated $f_{sw}$ harmonics for rectangular pulse trains. This assumption in fact is incorrect because $V_{ens}$ spectrum highly differs from $V_{LISN}$ spectrum (see Fig.5 and Fig.6). That is why in this paper we will consider not only $A$ but also attenuation ($A_{EMI}$) of amplitudes of unmodulated $f_{sw}$ harmonics for $V_{LISN}$. So to calculate the attenuations the following equations will be used

$$A = 20\log_{10}(\max|S_{Vens}(f)| / \max|S_{Vens1}(f)|)\,, \qquad (12)$$

$$A_{EMI} = 20\log_{10}(\max|S_{VLISN}(f)| / \max|S_{VLISN1}(f)|)\,, \qquad (13)$$

where $S_{Vens}$ and $S_{Vens1}$ are unmodulated and SFM $V_{ens}$ spectra, but $S_{VLISN}$ and $S_{VLISN1}$ are unmodulated and SFM $V_{LISN}$ spectra. To calculate the attenuations for sinusoidal SFM (4), (6), (12) and (13) should be used, but for sawtooth and triangular SFM (4), (7), (10)-(13) can be used. Calculated $A$ and $A_{EMI}$ as a function of $\Delta f_{sw}$ ($f_m$=const) for different $f_{sw}$ and $m(t)$ are shown in Fig.7.

The results clearly show that conducted EMI attenuation cannot be characterized by the parameter $A$ (as it was done in numerous papers), because the actual conducted EMI attenuation ($A_{EMI}$) highly differs from $A$. Moreover $A$ depends only on $\Delta f_{sw}$, $f_m$ and $m(t)$, but $A_{EMI}$ depends also on $f_{sw}$ value. So when calculating conducted EMI attenuation due to SFM, $f_{sw}$ should also be taken into account. Moreover $A$ is an increasing function of $\Delta f_{sw}$, but $A_{EMI}$ increases, then it achieves its maximum and then it even decreases as $\Delta f_{sw}$ increases (see Fig.7). Since the 1st sideband amplitude is the highest in SFM $V_{LISN}$ spectrum and $f_{sw}$ set the location of the sideband in the frequency range, then when the 1st sideband is in the range where $K_{EMI}(f)$ changes slowly, difference $\Delta A$ between $A$ and $A_{EMI}$ is minimal (this mainly corresponds to the high frequency range). However when the 1st sideband is in the range where $K_{EMI}(f)$ changes steeply, the difference $\Delta A$ is high (this mainly corresponds to low frequency range). Approximate $\Delta A$ can be calculated using the following simple expression

$$\Delta A \approx \max\left[ \begin{matrix} \left| |\underline{K}_{EMI}(f_{sw\min})| - |\underline{K}_{EMI}(f_{sw})| \right| \\ \left| |\underline{K}_{EMI}(f_{sw\max})| - |\underline{K}_{EMI}(f_{sw})| \right| \end{matrix} \right], \qquad (14)$$

where $f_{swmax}= f_{sw}+\Delta f_{sw}$. For rather small values of $\Delta f_{sw}$ (up to 10 kHz) $A$ is approximately equal to $A_{EMI}$, however the higher is $\Delta f_{sw}$ the higher also is $\Delta A$.

It is interesting to observe from Fig.7 that $A_{EMI}$ for sawtooth SFM is the highest but for sinusoidal it is the lowest, that is why it is better to use sawtooth $m(t)$.

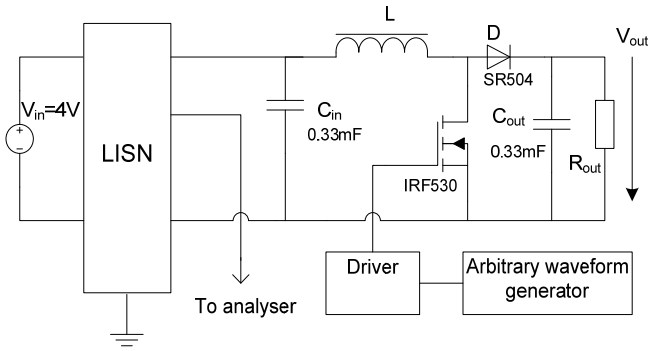


Fig.8. Simplified schematic diagram of the experimental setup.

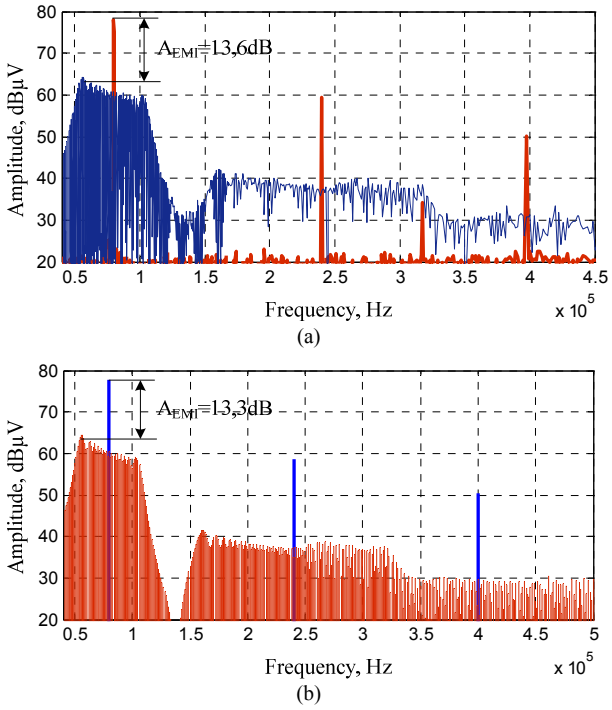


Fig.9. Experimental (a) and theoretical (b) spectra of $V_{LISN}$ spectrum with and without SFM. SFM parameters: $\Delta f_{sw}$=30kHz, $f_m$=1kHz, $f_{sw}$=80kHz, *m(t)* sawtooth. Other parameters: $C_h$=0pF, $V_{out}$=8V; RBW=200Hz.

As for the choice of modulation frequency, it is widely known that to get acceptable EMI reduction $f_m$ should be chosen slightly higher than RBW (which is usually set by a standard, e.g. CISPR 22) [10]. The most problematic SFM parameter to choose is $\Delta f_{sw}$. When designing SFM SMPC $\Delta f_{sw}$ should be carefully chosen so that $A_{EMI}$ is maximal. The derived expressions can be used for this purpose.

## IV. Experimental Verification

### A. Experimental setup

Experimental boost SMPC (Fig.8) operating in CCM is tested in an open loop mode to verify the theoretical analysis described above. In the experiments a regulated DC source is connected to the input of the boost SMPC. The input voltage of the boost converter is $V_{in}$=4 V; output load 12Ω and $f_{sw}$=80 kHz. For the experiments MOSFET IRF530 was used without external heatsink, so only differential mode conducted EMI will be considered in the calculations. To perform SFM, a frequency modulated square waveform signal from an arbitrary waveform generator is fed into the driver controlling the power MOSFET. The necessary SFM parameters can be set using the generator.

### B. Experimental results

Conducted EMI ($V_{LISN}$ spectrum) is analyzed using a spectrum analyzer (Agilent E4402B) with RBW=200Hz and a peak detector. The experimental and calculated $V_{LISN}$ spectra are depicted in Fig.9. As it can be seen the difference between the results is not high. Thus the derived expressions can be used for the conducted EMI calculation.

## V. Procedure for the Choice of SFM Parameters

To get the maximum EMI attenuation due to the use of SFM for the given value of $f_{sw}$, SFM parameters should be properly chosen. For this purpose a procedure for the choice of optimum SFM parameters to get maximum EMI attenuation is proposed as follows:

step 1: choose $f_m$ slightly higher than RBW;
step 2: as *m(t)* choose sawtooth;
step 3: calculate unmodulated $V_{LISN}$ spectrum using (1)-(5);
step 4: calculate SFM $V_{LISN}$ spectrum using (1)–(4), (7), (10);
step 4: calculate $A_{EMI}$ versus $\Delta f_{sw}$ using (13);
step 5: find $\Delta f_{swmax}$ at which $A_{EMI}$ is at maximum;
step 6: choose $\Delta f_{sw}$= $\Delta f_{swmax}$;
step 7: end.

## VI. Conclusions

The comprehensive theoretical analysis presented in this paper shows that the assumption that conducted EMI attenuation ($A_{EMI}$) due to the use of SFM depends only on modulation index and modulation waveform (as it was considered by other researchers) generally is incorrect. $A_{EMI}$ depends not only on $\Delta f_{sw}/f_m$ and *m(t)*, but also on $f_{sw}$. This is because in the analysis LISN, input filter and power inductor parameters should be taken into account.

The derived expressions to numerically calculate conducted EMI spectrum and attenuation in SFM SMPC can be very useful in the design process, because they require less computation time than FFT.

The presented analysis shows that sawtooth modulation waveform is the best choice. The most problematic SFM parameter to choose is $\Delta f_{sw}$. When designing a SFM SMPC $\Delta f_{sw}$ should be carefully chosen so that $A_{EMI}$ is at maximum. For this purpose the derived expressions can be used. The developed procedure for the choice of SFM parameters can simplify the selection of optimum SFM parameters to get maximum EMI attenuation for the given value of $f_{sw}$.

## Acknowledgments

This research was funded by a grant (No. 467/2012) from the Latvian Council of Science.

## REFERENCES

[1] C. R. Paul, Introduction to Electromagnetic Compatibility. New Jersey: John Wiley & Sons, 2nd ed., 2006, pp. 49-90.

[2] F. Zare, "EMI issues in modern power electronic systems," *IEEE EMC Society Newsletter*, No.221, pp.66-70, 2009.

[3] K. Mainali, R. Oruganti, "Conducted EMI Mitigation Techniques for Switch-Mode Power Converters: A Survey," *IEEE Transactions on Power Electronics*, vol. 25, no. 9, pp. 2344-2356, 2010.

[4] G. M. Dousoky, M. Shoyama, T. Ninomiya, "Double-hybrid spread-spectrum technique for conducted-EMI reduction in DC-DC switching regulators with FPGA-based controller," *IEEE Telecommunications Energy Conference, 2009 (INTELEC 2009)*, pp. 1-6.

[5] S. Johnson and R. Zane, "Custom spectral shaping for EMI reduction in high-frequency inverters and ballasts," *IEEE Transactions on Power Electronics,* vol. 20, no.6, pp. 1499 – 1505, Nov. 2005.

[6] D. Gonzalez, J. Balcells, A. Santolaria, J. Bunetel, J. Gago, D. Magnon, S. Brehaut, "Conducted EMI Reduction in Power Converters by Means of Periodic Switching Frequency Modulation," *IEEE Transactions on Power Electronics*, vol.22, no.6, pp. 2271-2281, 2007.

[7] K. Tse, H. Chung, S. Hui, H. So, "Comparative Study of Carrier-Frequency Modulation Techniques for Conducted EMI Suppression in PWM Converters," *IEEE Transactions on Industrial Electronics*, vol. 49, no.3. pp. 618-627, 2002.

[8] J. Balcells, A. Santolaria, A. Orlandi, D. Gonzalez, and J. Gago, "EMI reduction in switched power converters using frequency modulation techniques," IEEE Trans. Electromagn. Compat., vol. 47, no. 3, pp. 569–576, Aug. 2005.

[9] Santolaria A., SSCG methods of EMI emissions reduction applied to switching power converters // Ph.D. dissertation, Electron. Eng. Dept., Polytechnic University of Catalonia, Barcelona, Spain, Jul. 2004.

[10] F. Lin and D. Y. Chen, "Reduction of power supply EMI emission by switching frequency modulation," IEEE Trans. Power Electron., vol. 9, no. 1, pp. 132–137, Jan. 1994.

[11] K.B. Hardin, J.T. Fessler, D.R. Bush, "Spread Spectrum Clock Generation for the Reduction of Radiated Emissions," *Proceedings of IEEE International Symposium on Electromagnetic Compatibility*, August 1994, pp. 227-231.

[12] P. Musznicki, JL. Schanen, P. Granjon, P.J. Chrzan, "Better understanding EMI generation of power converters," *Proceedings of IEEE Power Electronics Specialists Conference (PESC2005)*, Recife, Brazil, June 2005, pp. 1052-1056.

[13] F. Giezendanner, J. Biela, J. W. Kolar, S. Zudrell-Koch, "EMI noise prediction for electronic ballasts," *IEEE Transactions on Power Electronics*, vol. 25, no. 8, pp. 2133-2141.

[14] S. Wang, F.C. Lee, W.G. Odendaal "Improving the performance of boost PFC EMI filters," *Proceedings of IEEE Applied Power Electronics Conference and Exposition (APEC 2003)*, Feb. 2003, pp. 368–374.

[15] L. Yang, B. Lu, W. Dong, Z. Lu, M. Xu, F.C. Lee, W.G. Odendaal "Modelling and characterization of a 1 KW CCM PFC converter for conducted EMI prediction," *Proceedings of IEEE Applied Power Electronics Conf. and Exposition (APEC 2004)*, 2004, pp. 763–769.

[16] K. Mainali, R. Oruganti, "Simple analytical models to predict conducted EMI noise in a power electronic converter," *Proceedings of the 33rd Annual Conference of the IEEE Industrial Electronics Society (IECON2007)*, 2007, pp. 1930–1936.

[17] K. Kostov, J.-P. Sjöroos, J. Kyyrä, and T. Suntio "Selection of Power Filters for Switched Mode Power Supplies," *Proceedings of Nordic Workshop on Power and Industrial Electronics (NORPIE 2004)*, Trondheim, Norway, June 2004, pp. 1-7.

[18] L. Barragan, D. Navarro, J. Acero, I. Urriza, and J-M. Burdío, "FPGA Implementation of a Switching Frequency Modulation Circuit for EMI Reduction in Resonant Inverters for Induction Heating Appliances," *IEEE Transactions on Industrial Electronics*, vol. 55, no.1, Jan. 2008, pp. 11 – 20.

**Deniss Stepins** received the B.Sc., M.Sc. and Dr.Sc.Ing degrees in electronics from Riga Technical University, Riga, Latvia, in 2004, 2006 and 2011 respectively.

He is currently a researcher and lecturer in the Department of Radioelectronics, Riga Technical University. He has been involved in several research projects on the examination of spread spectrum technique for switching power converters and improvement of power magnetic components. His research interests include EMI reduction techniques applied to switching power converters, control of switch-mode power converters and planar magnetic components.

He is currently an IEEE member.

Postal address: Department of Radioelectronics, Riga Technical University, LV-1048, 12 Azenes street, Riga, Latvia.

e-mail: deniss.stepins@rtu.lv.